Simulation results for the three types of channel were produced, for excitation signal levels varying between 0 and −60 dBm. Once the simulation data were obtained, the MLP was trained with the data and its synaptic weights were frozen (Fig. 3). The channel identification system was then tested with 2000 randomly selected sets of preprocessed data from simulated linear, A-law and ADPCM channels.

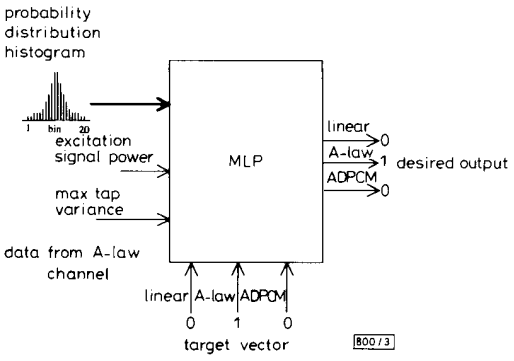

Fig. 3 *Training the multilayer perceptron*

Choosing the optimum MLP structure: The back-propagation algorithm of Rumelhart *et al.* [5] has been widely used in the training of MLPs. However, for different applications, the back-propagation algorithm may be modified slightly. In this simulation, the MLP learning rate ε, and momentum term α, were adaptable [5]. Owing to the large number of permutations of the MLP variables, it was not possible to try every combination of parameters. Instead, the MLP parameters were adjusted to give the best performance, and then the parameters were varied about this norm. To achieve this, first the structure was changed, by varying the number of processing layers and elements. The most effective was found to be a three layer network, with an input layer of 22 nodes, a hidden layer of 66 nodes, and an output layer of three nodes. Secondly, the adaptation parameters of the MLP were varied to further increase the performance of the classifier. The momentum term α was varied to find its optimum value, and was found to be 0·95.

Results: The results of the simulations are given in Table 1. These results are with the MLP using the logistic activation function, sum squares error measurement and no adaptation of the learning rate or momentum term [5]. The standard deviation of the Gaussian noise added to MLP weights during training was 0·45, and the momentum parameter $\alpha = 0{\cdot}95$.

Table 1 SIMULATION RESULTS

Learning rate ε	Channel type	% correctly identified
0·025	Linear	95
	A-law	86
	ADPCM	91
0·05	Linear	97
	A-law	86
	ADPCM	92
0·075	Linear	91
	A-law	83
	ADPCM	97
0·10	Linear	94
	A-law	83
	ADPCM	87

Conclusions: It can be seen from the results of the simulations, that the method of channel identification described works in the limited context of the simulation environment. However, more work is needed to further develop and verify this method of channel identification. Suggestions for further work include:

(i) making the simulation more realistic by including effects seen on real telephone lines, such as impulsive switch noise, crosstalk, and the effects of analogue to digital conversion; this would give an indication of whether the process described in this Letter is robust enough to use on real telephony channels

(ii) trying to improve the accuracy of the classification process by:

(*a*) using other adaptive filter parameters in the classification vector, such as higher order moments of the variance

(*b*) using different MLP training strategies

(*c*) using other classifiers such as the Mahalanobis classifier or the radial basis function

(iii) expanding the training data to include other coding schemes, such as sub-band coders, LPC coders, multiple ADPCM hops, etc.; this would give the system the ability to recognise more types of channel

(iv) the work could take a more theoretical viewpoint by attempting to classify specific nonlinearities such as square and cube law, or the more general Volterra series nonlinearity; this would help establish the theoretical limitations of the channel identification process.

© IEE 1993
21st April 1993

D. M. Alley (*Signal Processing Section, BT Laboratories, Martlesham Heath, Ipswich, United Kingdom*)

References

1 EYKHOFF, P.: 'System identification. Parameter and state estimation' (Wiley Interscience series, 1974)
2 CCITT Blue Book Volume III Fascicle III.4 General Aspects of Digital Transmission Systems; Terminal Equipments, Recommendation G711, November 1988
3 CCITT Blue Book Volume III Fascicle III.4 General Aspects of Digital Transmission Systems; Terminal Equipments, Recommendation G721, November 1988
4 RUMELHART, D. E., HINTON, G. E., and WILLIAMS, R. J.: 'Learning internal representations by error propagation', *in* 'Parallel distributed processing' (MIT Press, Cambridge, MA, 1987), Chap. 8
5 ALLEY, D. M.: 'Network topology identification from measured channel impairment data'. MSc Thesis, Dept. of Electronic Systems Engineering, University of Essex, Colchester, 1992

THICKNESS DETERMINATION OF POLY-Si/POLY-OXIDE/POLY-Si/SiO_2/Si STRUCTURE BY ELLIPSOMETER

T. S. Chao, C. L. Lee and T. F. Lei

Indexing terms: Measurement, Thin films, Ellipsometry

An ellipsometry measurement method is proposed to measure the poly-Si/poly-oxide/poly-Si/SiO_2/Si structure. The thickness of each layer in this structure can be easily obtained by a conventional ellipsometry measurement. The measured result is consistent with that of cross-sectional TEM.

Introduction: Polycrystalline silicon (poly-Si) films have been widely used in integrated circuits as gate electrodes, masks for impurity implantation, interconnections, and the poly-emitter of high-performance bipolar transistors [1, 2]. The poly-Si/poly-oxide/poly-Si/SiO_2/Si structure is used frequently in fabrication of capacitors and thin film transistor (TFT) devices. The thickness of each layer in this structure is of concern because different thicknesses result in different electrical characteristics.

In measuring the thickness and the optical properties of poly-Si, an ellipsometer is usually used [3]. However, there

are some problems which make the measurement either difficult or inaccurate. Generally, the poly-Si is a lightly absorbing film which introduces an imaginary part to its refractive index. Hence, it needs more than two measurements such as multiple incidence angle or wavelength to solve this problem. We have proposed a multiple-angle incident ellipsometry method and a sandwich structure [4]. In this work, a special method for measuring the complex structure is proposed for the conventional ellipsometer measurement with a single incidence angle (70·0°) and a single incidence wavelength (632·8 nm) to measure the thickness of each layer.

Experiment: Fig. 1 shows the structure of a stacked poly-Si(II)/poly-oxide/poly-Si(I)/SiO_2/Si structure. In experiments, a bottom SiO_2 layer was first grown about 3200 Å and etched

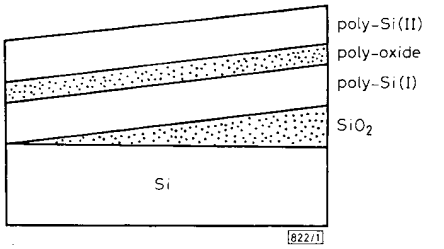

Fig. 1 *Poly-Si(II)/poly-oxide/poly-Si(I)/SiO_2/Si structure for ellipsometry measurement*

by HF : H_2O = 1 : 50 as a bevelled surface. Poly-Si(I) film was then deposited by the low pressure chemical vapour deposition (LPCVD) method at 550°C for 75 min with N_2 annealing at 1000°C for 30 min. The poly-Si(I) film was thermally oxidised in dry O_2 ambient at 1000°C for 30 min. Finally, the poly-Si(II) was deposited at 550°C for 25 min and with N_2 annealing at 900°C for 30 min. An ellipsometer was used to measure along the bevelled sample surface. Measured (Δ, ψ) data were obtained corresponding to different bottom oxide thicknesses. These measured (Δ, ψ) data were then put into a fitting program to fit the value of thickness for each layer. To reduce the complexity for too many unknown parameters, the refractive indices of poly-Si (Si) and poly-oxide (SiO_2) are given as 3·858 − i0·018 and 1·46, respectively [5]. Under this condition, the remaining unknown parameters are the thickness of Tpoly-Si(II), Tpoly-oxide, and Tpoly-Si(I). The thickness of the bottom oxide can be changed during the simulation. The process for finding the solution is as follows. First, Tpoly-Si(I), Tpoly-oxide, and Tpoly-Si(II) are given a reasonable value. The thickness of bottom oxide changes from 0 to 2830 Å which is the cycle period of the oxide. This produces a loop in the (Δ, ψ) data and the simulated (Δ, ψ) curves can be calculated. The values of Tpoly-Si(I), Tpoly-oxide, and Tpoly-Si(II) are then varied over a range to obtain the minimum error for finding the best fitted exact thickness of each layer.

In Fig. 2, dotted points are the measured data (Δ, ψ), and the solid lines are the simulated curves for different thicknesses of poly-Si(I) from 1290 Å (line 1) to 1330 Å (line 5) with fixed thickness of Tpoly-oxide 400 Å, and Tpoly-Si(II), 510 Å. It is easy to see that the best fitted thicknes of poly-Si(I) is line 3 of thickness 1310 Å. In fact, the fitting error for line 3 is also a minimum. Using this method, the thickness for each layer can be calculated. The best fitted thicknesses are 1310, 400, and 510 Å for Tpoly-Si(I), Tpoly-oxide, and Tpoly-Si(II),

Table 1 THICKNESS OF POLY-Si(II)/POLY-OXIDE/POLY-Si(I)/SiO_2/Si STRUCTURE MEASURED BY ELLIPSOMETRY AND TEM

	Ellipsometry	TEM
Poly-Si(I) Å	1310	1200 ± 33
Poly-oxide Å	400	460 ± 33
Poly-Si(II) Å	510	500 ± 33

respectively. These results are compared with those obtained by using cross-sectional TEM. Fig. 3 shows the cross-sectional

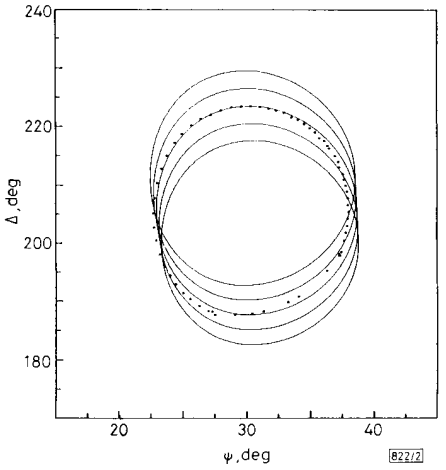

Fig. 2 *Measured data of Δ and ψ and simulated data for different thickness of poly-Si(I) from 1290 Å (line 1) to 1330 Å (line 5) with fixed thickness Tpoly-oxide, 400 Å, and Tpoly-Si(II), 510 Å*

····· measured
——— simulated
Line 1: top ring
Line 5: bottom ring

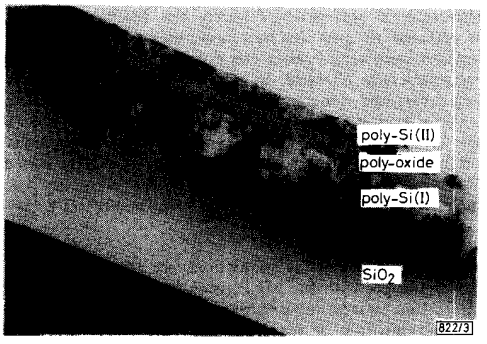

Fig. 3 *Cross-sectional TEM photograph of poly-Si(II)/poly-oxide/poly-Si(I)/SiO_2/Si structure (50 K × 3)*

TEM of the poly-Si(II)/poly-oxide/poly-Si(I)/SiO_2/Si structure. It can be seen that the interface of poly-Si/SiO_2 is not very smooth. The thicknesses measured by the ellipsometer are close to that of cross-sectional TEM; the values of Tpoly-Si(I), Tpoly-oxide, Tpoly-Si(II) are estimated as 1200 ± 33, 460 ± 33, and 500 ± 33 Å, respectively.

Conclusion: In conclusion, the thickness of each layer of the poly-Si(II)/poly-oxide/poly-Si(I)/SiO_2/Si structure can be easily obtained by a conventional single incidence angle and single incidence wavelength ellipsometer. The measured results are very close to those obtained by cross-sectional TEM.

Acknowledgments: This work is supported by National Science Council of ROC through the contract of NSC-80-0404-E009-48.

© IEE 1993
23rd April 1993

T. S. Chao (*National Nano Device Laboratory, 1001-1 Ta Hsueh Rd., Hsinchu 30050, Taiwan, Republic of China*)

C. L. Lee and T. F. Lei (*Department of Electronics and Engineering and Institute of Electronics, National Chiao Tung University, Hsinchu, Taiwan, Republic of China*)

References

1 WONG, C. Y., THOMPSON, C. V., and TU, K. N. (Eds.): 'Polysilicon films and interfaces' (Material Research Society, 1988)
2 KAMINS, T. (Ed.): 'Polycrystalline silicon for integrated circuit applications' (Kluwer Academic Publishers, 1988)
3 IRENE, E. A., and DONG, D. W.: 'Ellipsometry measurements of poly-Si films', *J. Electrochem. Soc.*, 1982, **129**, pp. 1347–1352
4 CHAO, T. S., LEE, C. H., LEI, T. F., and YEN, Y. T.: 'Poly-oxide/poly-Si/SiO_2/Si structure for ellipsometry measurement', *Electron. Lett.*, 1992, **28**, pp. 1144–1145
5 TOMPKINS, H. G., and VASQUEZ, B.: 'A special case of using ellipsometry to measure the thickness of oxide on poly-Si', *J. Electrochem. Soc.*, 1990, **137**, pp. 1520–1524

UNIVERSAL ACTIVE CURRENT FILTERS USING SINGLE SECOND-GENERATION CURRENT CONVEYOR

C.-M. Chang, C.-C. Chien and H.-Y. Wang

Indexing terms: Circuit theory and design, Active filters, Current conveyors

Two novel universal active current filters with a single second-generation current conveyor (CCII), which use fewer passive RC elements and have larger quality factor than the previous two filters proposed by the author, are presented.

Introduction: The first universal biquad [1] was designed by Nawrocki and Klein in 1986. Although the original design using operational transconductance amplifiers (OTAs) is most suitable for integration purposes due to the absence of resistors in the circuit, the performance limitations of OTAs such as poor bandwidth and poor output drive capability will restrict the overall operating performance. High-performance current conveyors (CCs) have become an attractive alternative to OTAs in this application because of their higher bandwidths and improved current drive capabilities. Toumazou and Lidgey [2] then presented a universal active biquad network with CCs based on the redesign of this OTA realisation. Singh and Senani [3] subsequently presented a simpler active-RC configuration which uses only three current conveyors and realises all standard voltage-mode biquads.

In 1989, Roberts and Sedra proposed that the circuits based on current amplifiers operate at higher signal bandwidths, with greater linearity, and larger dynamic range than their voltage-based circuit counterparts [4]. Hence, three universal active biquads were presented [5–7] with current gain using OTAs, CCs, and a single CC, respectively. This Letter presents two novel universal active current biquads which have a simpler structure and larger quality factor than the previous biquad [7] proposed by the author.

Circuit description: The first proposed network, based on and employing a minus-type second-generation current conveyor (CCII−), is shown in Fig. 1. Using standard notation, the port relations of a CCII− current conveyor can be characterised by [8]

$$\begin{bmatrix} i_y \\ v_x \\ i_z \end{bmatrix} = \begin{bmatrix} 0 & 0 & 0 \\ 1 & 0 & 0 \\ 0 & -1 & 0 \end{bmatrix} \begin{bmatrix} v_y \\ i_x \\ v_z \end{bmatrix} \quad (1)$$

The current transfer functions for the network of Fig. 1 are given by the following equations:

$$I_0/I_i = \{s^2 C_2 C_5 + s[C_5 G_3 - C_2(sC_4 + G_4)] + G_1 G_3\}/\Delta \quad (2)$$

$$I'_0/I_i = sC_2 G_4/\Delta \quad (3)$$

$$I''_0/I_i = s^2 C_2 C_4/\Delta \quad (4)$$

where $\Delta = s^2 C_2 C_5 + sG_3(C_2 + C_5) + G_1 G_3$.

The two output currents I'_0 and I''_0, taken out through another CCII− with a virtual ground on input, give the bandpass and highpass signals, respectively. From eqn. 2 we see three possible cases:

(*a*) *Notch filter:* In eqn. 2, if $C_4 = 0$ and $G_4 = C_5 G_3/C_2$, this results in a notch transfer function.

(*b*) *Allpass filter:* In eqn. 2, if $C_4 = 0$ and $G_4 = (2C_5 G_3 + C_2 G_3)/C_2$, this results in an allpass transfer function.

(*c*) *Lowpass filter:* In eqn. 2, if $C_4 = C_5$ and $G_4 = C_5 G_3/C_2$, this results in a lowpass transfer function.

Note that we can adjust the grounded resistor R_4 and the grounded capacitor C_4 and then obtain second-order current-mode lowpass, highpass, bandpass, notch and allpass signals. The resonance angular frequency ω_0 and quality factor Q of eqns. 2–4 are

$$\omega_0 = (G_1 G_3/C_2 C_5)^{1/2} \quad (5)$$

and

$$Q = (G_1/G_3)^{1/2}(C_2 C_5)^{1/2}/(C_2 + C_5) \quad (6)$$

Note that the magnitude of Q can be larger than 1/2. The sensitivities of ω_0 and Q to passive components are

$$S_{G_1}^{\omega_0} = S_{G_3}^{\omega_0} = -S_{C_2}^{\omega_0} = -S_{C_5}^{\omega_0} = S_{G_1}^{Q} = -S_{G_3}^{Q} = 1/2$$

$$S_{C_2}^{Q} = \frac{1}{2} - \frac{C_2}{C_2 + C_5}$$

and

$$S_{C_5}^{Q} = \frac{1}{2} - \frac{C_5}{C_2 + C_5}$$

all of which are small.

The second proposed network, employing one resistor more than the first one shown in Fig. 1, is shown in Fig. 2. The

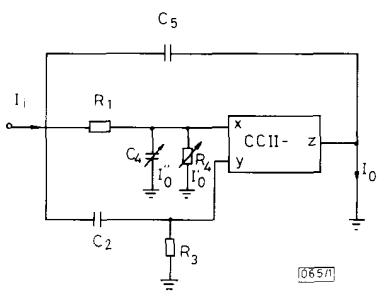

Fig. 1 *First proposed universal active current filter using single CCII−*

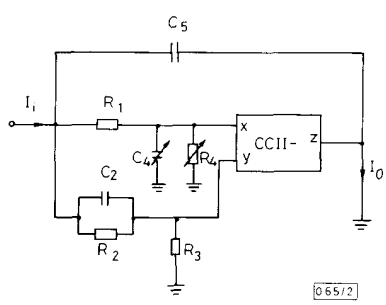

Fig. 2 *Second proposed universal active current filter using single CCII−*